scientific reports

Check for updates

OPEN

Endothelial soluble guanylate cyclase enzyme inhibitors as a novel target for the treatment of sepsis-related hypotension

Yousif Ali Ahmed Suleiman[1], Abuzor Mohamed Mohyeldin Khalil[2] & Yassir A. Almofti[3]✉

Sepsis-related hypotension is a life-threatening condition due to systemic infection leading to widespread inflammation and blood vessel dilation. This can cause a dramatic drop in blood pressure, impairing blood flow to vital organs and potentially leading to organ failure and death. NO was recognized as a significant factor in sepsis in 1990 and became an important therapeutic target. NO plays a dual role in sepsis, exhibiting both beneficial and harmful effects. Inhibiting sGC may help reduce the excessive vasodilation associated with sepsis-induced vasoplegia. This study utilized CADD to screen over 320 naturally occurring compounds from the PubChem database for potential sGC inhibitors. A comprehensive virtual screening process, which included protein–ligand docking, binding free energy calculations, and pharmacokinetic profiling, led to the identification of promising candidates such as Hypericin and Hypocrellin A2. These compounds demonstrated superior binding affinities and pharmacokinetic properties compared to existing inhibitors. Hypericin achieved a docking score of -14.232, indicating strong interactions with the receptor. It also exhibited favourable pharmacokinetic characteristics, including significant tissue-binding potential and stability within the binding pocket, as well as low predicted toxicity and a substantial safety margin. This research lays the groundwork for future in vitro and in vivo studies, which could improve Hypericin-based effective therapies for sepsis-induced vasoplegia and hypotension.

Keywords Nitric Oxide receptor inhibitor, Hypericin, Sepsis, Hypotension, Computational drug design

Sepsis is a complex immune mechanism and is described as a life-threatening dysfunction of vital organs caused by dysregulated host reactions to infections[1,2]. Sepsis is further characterised by systemic inflammatory response syndrome (SIRS), which represents an excessive production of inflammatory cytokines that activate body immunity[3]. Therefore, sepsis denotes a considerable clinical challenge associated with high mortality rates and substantial economic impact[4]. Estimating sepsis-related death is complex because of the controversy in clinical definitions, heterogeneous clinical signs of patients, different hospital-related coding systems for sepsis, and varying dimensions of sepsis-related public awareness. Therefore, every year, sepsis and septic shock cause millions of deaths worldwide, posing a major health challenge[5].

Septic shock is a critical sepsis state marked by low systemic vascular resistance, hypotension, high cardiac output and perfusion irregularities due to peripheral arteriolar vasodilation, resulting in harmful cellular and metabolic consequences with 50–75% mortality[6,7]. According to the guideline of The Society of Critical Care Medicine's Surviving Sepsis, systolic blood pressure of 100 mmHg or less is an indication of a quick Sequential Organ Failure Assessment score (qSOFA), which helps to identify patients with suspected sepsis infections[2]. Since hypotension exacerbates tissue perfusion, it is plausible that certain organ injuries can be prevented by maintaining a suitable arterial pressure. Preventing hypotension is, therefore, a vital component of sepsis management[8,9]. Excessive release of nitric oxide (NO), triggered by inducible nitric oxide synthase (iNOS), interleukin (IL)−1 and tumour necrosis factor (TNF), was identified as a crucial factor in sepsis-induced vascular relaxation hypotension in septic shock[10–13]. Sequential binding of NO to its primary receptor soluble guanylate cyclase ($_S$GC) on target endothelial cell membranes boosted the function of $_S$GC a 100-fold, leading to intracellular cGMP-induced pathophysiology of vasoplegia, promoting vasorelaxation[14–16]. In addition, activating $_S$GC in mice with severe sepsis showed reduced neutrophil migration and increased leukocyte sequestration into lung

[1]Al Adan Hospital, Hadiah Area, Al Ahmade Province, Kuwait City, Kuwait. [2]Department of Pharmacology, Faculty of Pharmacy, Sudan International University, Khartoum, Sudan. [3]Department of Biomedical Sciences, College of Veterinary Medicine, King Faisal University, Hufuf, Al-Ahsa, Saudi Arabia. ✉email: yamofti99@gmail.com

parenchyma tissues, culminating in lung failure and sepsis pneumonia in mice. Consequently, $_{S}$GC inhibition reduced the leukocyte sequestration with partially restoring the neutrophil accumulation into the pulmonary parenchyma[17]. In addition, inhibiting $_{S}$GC during the later stage of sepsis mitigated the excessive vasodilation link to sepsis-induced vasoplegia, resulting in decreased mortality in mic[18]. The iNOS-dependent suppression of $_{S}$GC has also been documented as a protective mechanism against TNF-induced fatal shock, bradycardia, and hypotension[19]. However, developing $_{S}$GC inhibitors faces challenges in finding specific compounds with favourable pharmacokinetics and low toxicity. Recently, computer-aided drug design (CADD) has facilitated the efficient identification of potential inhibitors from large chemical libraries, proving effective in various therapeutic areas.

In this study, we employed CADD to screen over 320 naturally occurring compounds from the PubChem database for potential $_{S}$GC inhibitors. Using a comprehensive virtual screening pipeline that included protein–ligand docking, binding free energy calculations, and pharmacokinetic profiling, we identified promising candidates like Hypericin and Hypocrellin A2, which showed better binding affinities and pharmacokinetic properties than existing inhibitors. Hypericin (4,5,7,4′,5′,7′-hexahydroxy-2,2′-dimethylnaphtodianthrone) and Hypocrellin A2 (3,10-xylene-4,9-anthracene derivative) are naturally occurring compounds which have broad pharmacological spectrum[20,21]. Hypericin achieved an impressive docking score of −14.232, indicating strong receptor interactions and compliance with Lipinski's rule of five, suggesting high drug-likeness. It also displayed favourable pharmacokinetic traits, including high tissue-binding potential and stability in the binding pocket, along with low predicted toxicity and a high safety margin. The findings highlight hypericin as a promising therapeutic candidate for overcoming the limitations of conventional inhibitors. This study provides a foundation for further in vitro and in vivo investigations, with the potential to advance effective treatments for sepsis-induced vasoplegia.

Method

Ligand database selection and preparation

A focused library of 320 natural compounds was curated from the PubChem database (https://pubchem.ncbi.nlm.nih.gov/). Ligands were selected based on reported bioactivity against cardiovascular or inflammatory pathways (literature references and PubChem bioassay records) compliance with Lipinski's rule of five for drug-likeness, structural diversity to cover a broad chemical space. These compounds were initially obtained in SDF format and subsequently converted into 3D structures using Open Babel software. Their corresponding 2D representations were sourced from the PubChem database (https://pubchem.ncbi.nlm.nih.gov/). Ligand preparation, structural format conversions, and geometry optimization were carried out using Open Babel version 3.1.1.

Protein preparation

The crystal structure of human sGC UniProt ID: Q02153 was retrieved from the uniport. Receptor grid generation was performed using AutoDock Tools version 1.5.6, employing a blind docking approach to enable ligand interaction across the entire surface of the protein. The grid box dimensions were configured to cover the complete receptor, allowing for the exploration of potential novel binding sites center_x = 100.111, center_y = 108.493, center_z = 122.845, size_x = 126, size_y = 42, size_z = 50.

Molecular docking

Molecular docking was performed using AutoDock Vina version 1.2.3. Custom configuration files were created with specific protein–ligand parameters to ensure precise estimation of binding affinities. After docking, the strength of the interactions and binding profiles were evaluated. Detailed protein–ligand interaction diagrams were then created and analysed using LigPlot + version 2.2.9.

Binding free energy calculations

To evaluate the stability and binding strength of the protein–ligand complexes, binding free energy was computed using the MM/GBSA (Molecular Mechanics/Generalized Born Surface Area) approach, executed through the gmx_MMPBSA tool, which integrates seamlessly with GROMACS 2025.1. The required topology (.tpr) and trajectory (.xtc) files were sourced from molecular dynamics simulations previously run in GROMACS. Protein and ligand groups were designated directly using the -cg flag, removing the necessity for generating a separate index file. The MM/GBSA calculations were directed by a configuration file (mmpbsa.in), set to process 100 frames taken at intervals of five frames, beginning with the first frame of the trajectory. The Generalized Born solvation model by Onufriev–Bashford–Case (igb = 5) was applied to simulate solvent effects implicitly, while per-residue energy breakdown (idecomp = 1) was activated to pinpoint amino acid residues significantly involved in ligand binding. Results, including total binding free energies and individual residue contributions, were extracted from the resulting.data output files.

Molecular dynamics simulations

Molecular dynamics (MD) simulations were carried out using the GROMACS software package. The topology file containing both the molecular structure and force field parameters was generated with the pdb2gmx utility using the Charmm36 force field. The system was solvated in a predefined simulation box filled with water molecules, and counterions were added via the editconf and genion tools to achieve overall charge neutrality. Initial energy minimization was performed using grompp and mdrun to eliminate steric clashes and ensure optimal geometry. The system was then equilibrated in two sequential stages: first under the NVT ensemble (constant number of particles, volume, and temperature) with temperature regulation via the V-rescale thermostat set at 300 K, followed by the NPT ensemble (constant number of particles, pressure, and temperature) using the Parrinello–Rahman barostat to maintain a pressure of 1 atm. During these equilibration phases, positional restraints were

applied to the protein to retain its structural stability. Electrostatic interactions were treated using the Particle Mesh Ewald (PME) method, with a cut-off distance of 10 Å for short-range interactions. The unrestrained production MD simulation was run for 10 ns, employing standard time-step integration and appropriate cut-off and constraint settings.

ADMET properties evaluation

The pharmacokinetic and toxicity profiles of the lead compounds were assessed using the SwissADME (http://www.swissadme.ch/index.php) and PROTOX-II (https://tox-new.charite.de/protox_II/) web servers. Parameters analysed included absorption, distribution, metabolism, excretion, toxicity (ADMET), drug-likeness, and bioavailability.

Results

In this study, we explored a set of naturally occurring SGCE (small GTPase-activating enzyme) inhibitors identified from the PubChem database, which listed over 320 potential compounds. Out of these, six were found to demonstrate significant binding affinity toward the SGCE enzyme. These six compounds include as shown in Fig. 1, Hypericin, Hypocrellin A2, Stictic Acid, Viola Styrene, and a standard ligand protein from the database, which was selected as a reference compound (control ligand) due to its documented efficacy and binding profile. The standard ligand was retrieved from PubChem and used as a control, showing a Ligand Efficiency Value (LVS) score of −14.232. This score provided a baseline for assessing the relative binding efficiency of the other selected ligands. However, docking score (binding affinity) is expressed in kcal/mol, whereas LVS is normalized per heavy atom and reported in kcal/mol per non-hydrogen atom. Unlike docking score, which represents the total binding energy, LVS allows fair comparison of ligands of different molecular sizes.

Although, after receptor-ligand interaction, we observed a notable increase in total polar surface area (TPSA) for the standard ligand, accompanied by an increase in the negativity of the LVS score to −14.03 as shown in Table 1. This enhanced negativity signifies a lower binding energy requirement and a higher affinity, indicating a strong tendency for receptor binding. The increased concentration of this ligand around the receptor suggests a propensity for significant tissue-protein binding, which may translate to an extensive volume of distribution and a prolonged elimination half-life (t½).

In comparison, Hypocrellin A2 emerged as a promising candidate with a high SlogP value of 4, indicative of moderate water solubility and a balance between hydrophilicity and lipophilicity. This characteristic enhances its bioavailability in plasma and facilitates renal excretion, likely resulting in a shorter t½. Upon binding, Hypocrellin A2 demonstrated a substantial increase in its radial plot from 546.5 to 646.5, with an LVS score of −12.953, only marginally lower than that of the standard ligand by approximately 2 points. This score, while slightly less favourable, still reflects a robust binding potential and suggests that Hypocrellin A2 is an effective candidate for further study.

Hypericin, a naturally occurring compound with PubChem ID 3663, demonstrated unique pharmacokinetic properties. Characterized by a narrow radial plot, high molecular weight, low lipophilicity, and an elevated TPSA, Hypericin is likely confined primarily to the intravascular compartment. This limited distribution is reflected in a shorter half-life and reduced volume of distribution. However, its LVS score of −14, closely aligning with the control ligand's score, marks it as a promising candidate for further evaluation in both in vitro and in vivo studies.

The comprehensive analysis of ligand binding and toxicity reveals that AG2P1001 and Hypericin exhibit the most favourable binding interactions and stability as depicted in Fig. 2. AG2P1001, the control ligand, demonstrates strong binding affinity with a stable MMGBSA score of −38.75, while Hypericin shows an even more favourable MMGBSA score of −40.36, suggesting comparable or superior binding stability, making it a promising candidate for both in vitro and in vivo studies. Hypocrellin A2 also displays strong binding as shown in Fig. 3, with an MMGBSA score of −37.44, though it is slightly less effective than AG2P1001 and Hypericin. However, its single hydrogen bond, as depicted in Fig. 4B, led us to select Hypericin as the leading candidate for further analysis. In contrast, Stictic Acid and Viola Styrene have lower binding affinities and stability, as indicated by MMGBSA scores of −32.76 and −34.62, respectively, suggesting weaker interactions with the receptor. Hypericin's toxicity profiling reveals potential interactions with cytochrome P450 (CYP) enzymes, particularly CYP1A2, CYP2C9, and CYP2C19, which may influence its pharmacokinetics and lead to drug-drug interactions. It exhibits moderate interactions with CYP3A4 and CYP2D6. It also has a predicted LD50 of 1000 mg/kg (Toxicity Class 4, GHS), indicating low toxicity, minimal nephrotoxicity, and low risks of neurotoxicity and carcinogenicity, making it promising for therapeutic use. Howbeit, we further conducted the analysis of the bond interactions as shown in Fig. 4. Molecular docking simulations were conducted to investigate the binding interactions of Hypericin and Hypocrellin A2 with the human soluble guanylate cyclase (sGC) β1 subunit. Both ligands occupied distinct yet functionally relevant binding pockets within the sGC structure, forming multiple non-covalent interactions that contribute to complex stability (Fig. 4). In the sGC–Hypericin complex (Fig. 4A), the ligand is embedded within the H-NOX domain (residues 1–194) of the β1 subunit, a domain critical for heme binding and nitric oxide (NO) sensing. Hypericin engages in several polar interactions and hydrogen bonds, most notably with His105, a residue essential for heme coordination. Additional interactions are observed with hydrophobic and aromatic residues such as Phe74, Met115, and Leu108, contributing to ligand anchoring via van der Waals and π-π stacking interactions. A key hydrogen bond (2.78 Å) with Tyr135 further stabilizes the complex. In contrast, the sGC–Hypocrellin A2 complex (Fig. 4B) reveals ligand binding in a regulatory region adjacent to the catalytic interface, spanning residues beyond the H-NOX domain. Hypocrellin A2 forms strong hydrogen bonds with Lys284 (3.16 Å) and Gln309 (2.92 Å), along with additional hydrophobic contacts involving residues such as Pro287 and Pro404. These interactions suggest

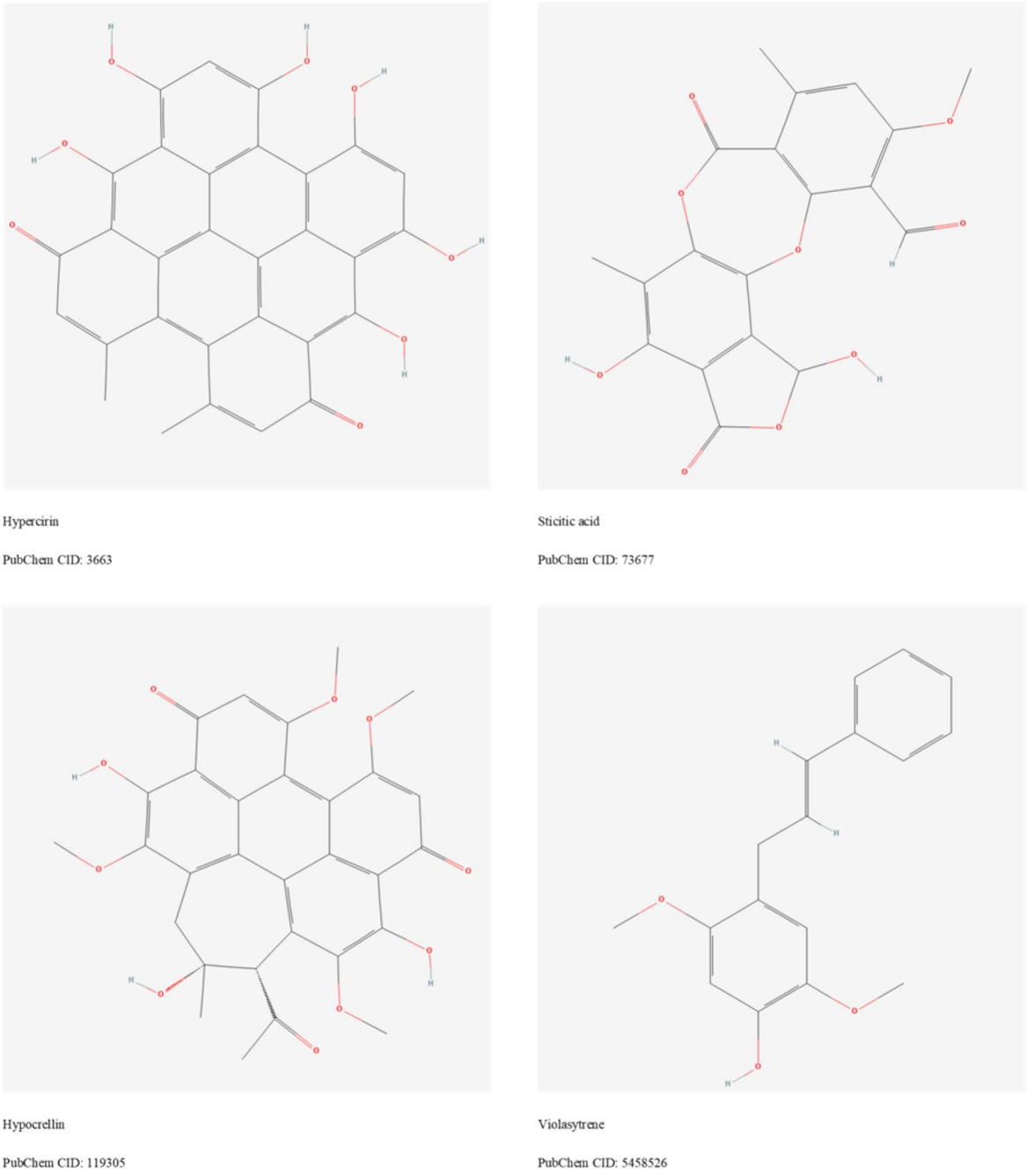

Fig. 1. Structures of the lead compounds.

a stabilizing role within a structurally flexible domain of sGC that mediates enzymatic activation and allosteric communication between subunits.

Molecular dynamic simulations

The figure presents molecular dynamics simulation analyses of the SGC enzyme bound to two different molecules: Hypericin and Hypocrellin.

RMSD (Root Mean Square Deviation): For SGC-Hypericin (A), the RMSD rises quickly and then stabilizes around 1.8–2.0 nm over 20,000 ps, indicating moderate structural deviation and suggesting some flexibility or instability in the complex. For SGC-Hypocrellin (D), the RMSD increases initially but then stabilizes at a much lower value (around 0.6–0.7 nm), depicting higher stability and less deviation compared to the Hypericin complex.

RMSF (Root Mean Square Fluctuation): The SGC-Hypericin complex (B) shows local fluctuations, especially for particular residues where RMSF peaks, with values ranging between 0.2 and 0.6 nm, indicating certain

Ligand	Slog-P	TPSA	LVS Score (kcal/mol per non-hydrogen atom)	MMGBSA (kcal/mol)
AG2P1001 (Undocked)	−16	114.9	-	-
AG2P1001 (Docked)	−16	3149	−14.03	−38.75
Hypocrellin A2 (Undocked)	4	148.8	-	-
Hypocrellin A2 (Docked)	4	148.8	−12.953	−37.44
Stictic Acid (Undocked)	2.7	128.6	-	-
Stictic Acid (Docked)	2.7	128.6	−8.817	−32.76
Viola Styrene (Undocked)	3.6	38.7	-	-
Viola Styrene (Docked)	16	38.7	−8.28	−34.62
Hypericin (Undocked)	5.6	155.5	-	-
Hypericin (Docked)	5.6	155.5	−14.351	−40.36

Table1. Comparative analysis of physicochemical properties, binding scores, and MMGBSA values of selected ligands in docked and undocked states.

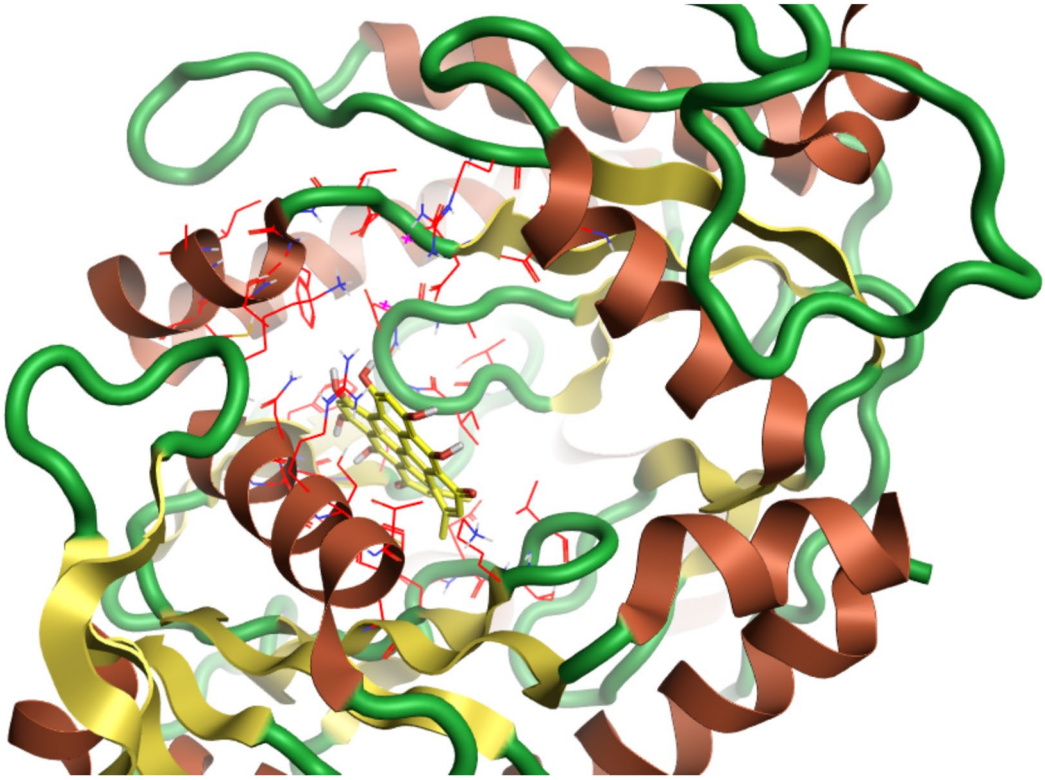

Fig. 2. Represents 3D of SGC enzyme bound to Hypericin molecule in it is active site. It is noticed that a golden molecule within the central part of the active binding site of our target protein with multiple aromatic rings more hydrogen bonds as well as weak electrostatic ones.

flexible regions. The SGC-Hypocrellin complex (E) displays overall lower RMSF values (generally < 0.5 nm), suggesting even less flexibility and more rigid binding, with fewer high-fluctuation residues.

Radius of Gyration (Rg): For SGC-Hypericin (C), the R.g starts high and gradually decreases, stabilizing at around 2.0 nm, pointing to a certain degree of structural compaction over the simulation. For SGC-Hypocrellin (F), the R.g remains steady throughout at about 2.5 nm, indicating persistent compactness and structural stability of the complex over the simulation period. However, Hypericin formed a higher number of stable hydrogen bonds (average 3.5, range 2–5) compared to Hypocrellin (average 2.0, range 1–3).(Fig. 5)

Discussion

Sepsis-induced vasoplegia remains a critical complication of sepsis, characterized by excessive nitric oxide (NO) production leading to profound vasodilation and multi-organ failure[22,23]. Current therapeutic options are limited, hence the urgent need for novel interventions. This study employs computer-aided drug design (CADD) to identify potential inhibitors of soluble guanylate cyclase (sGC), a key enzyme in the vasodilatory pathway.

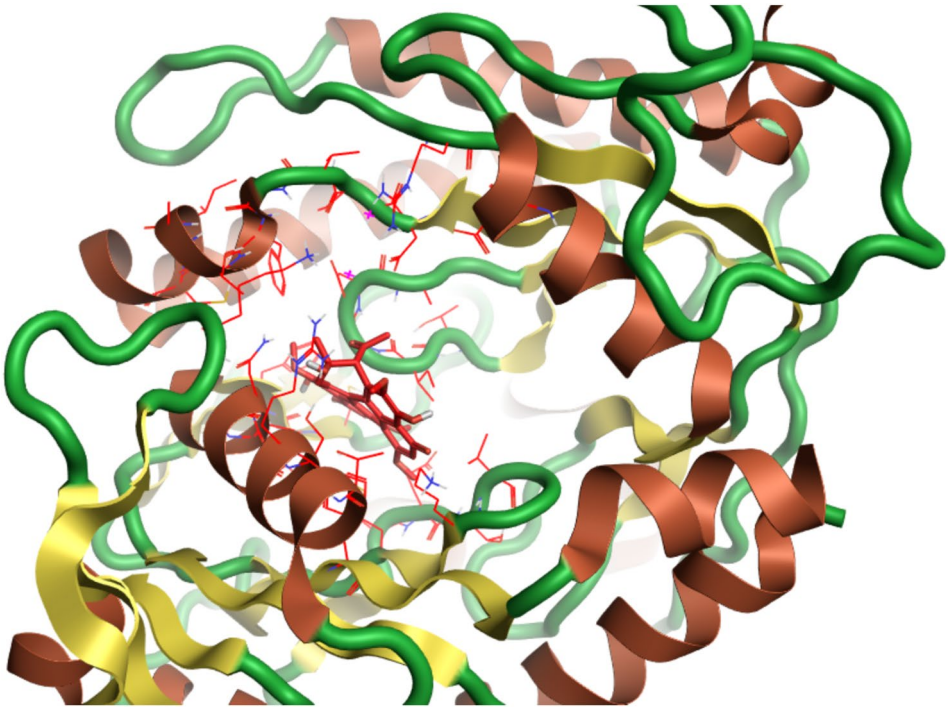

Fig. 3. Represents 3D view of SGC enzyme bound to Hypocrellin molecule in it is active site. It is noticed that Hypocrellin has multi aromatic rings and close to beta plated sheet of our enzyme with more hydrogen bonds as well as weak electrostatic forces which appeared blue in colour.

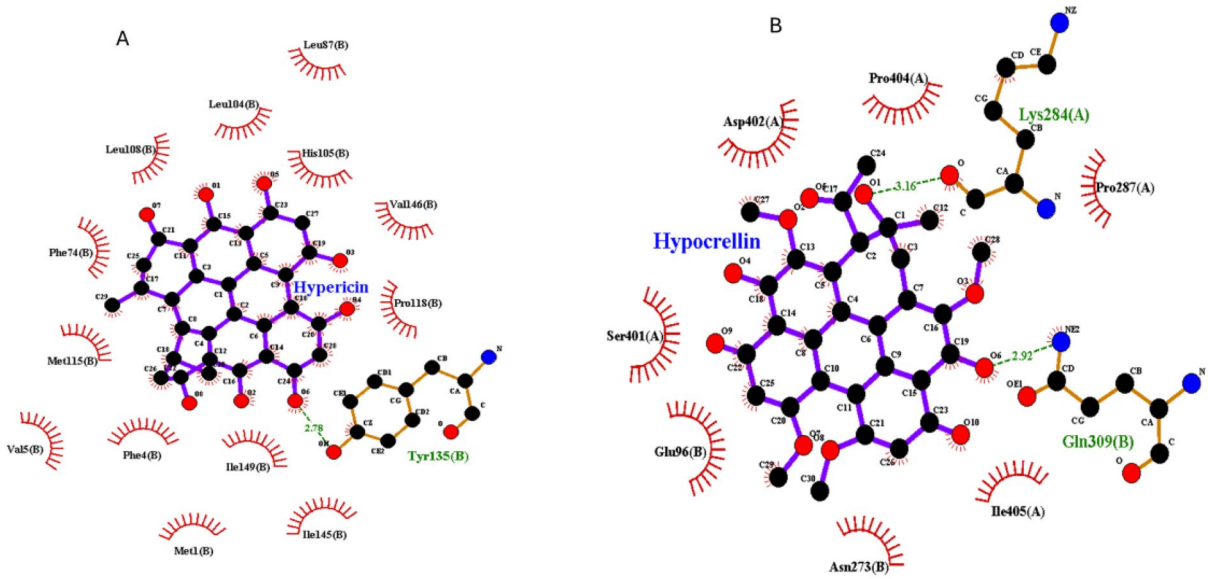

Fig. 4. Molecular Docking Interactions Illustrating the Stabilization of Complexes: (**A**) Hypericin with the sGC Enzyme and (**B**) Hypocrellin A2 with the sGC Enzyme, Highlighting Hydrogen Bond Interactions (green lines).

Based on reported bioactivity in cardiovascular and inflammatory pathways (as documented in literature and PubChem bioassay records), ligands were selected for their compliance with Lipinski's rule of five and structural diversity to ensure broad chemical space coverage. This rational filtering led to the identification of Hypericin and Hypocrellin A2 as lead candidates with strong predicted binding affinities for sGC.

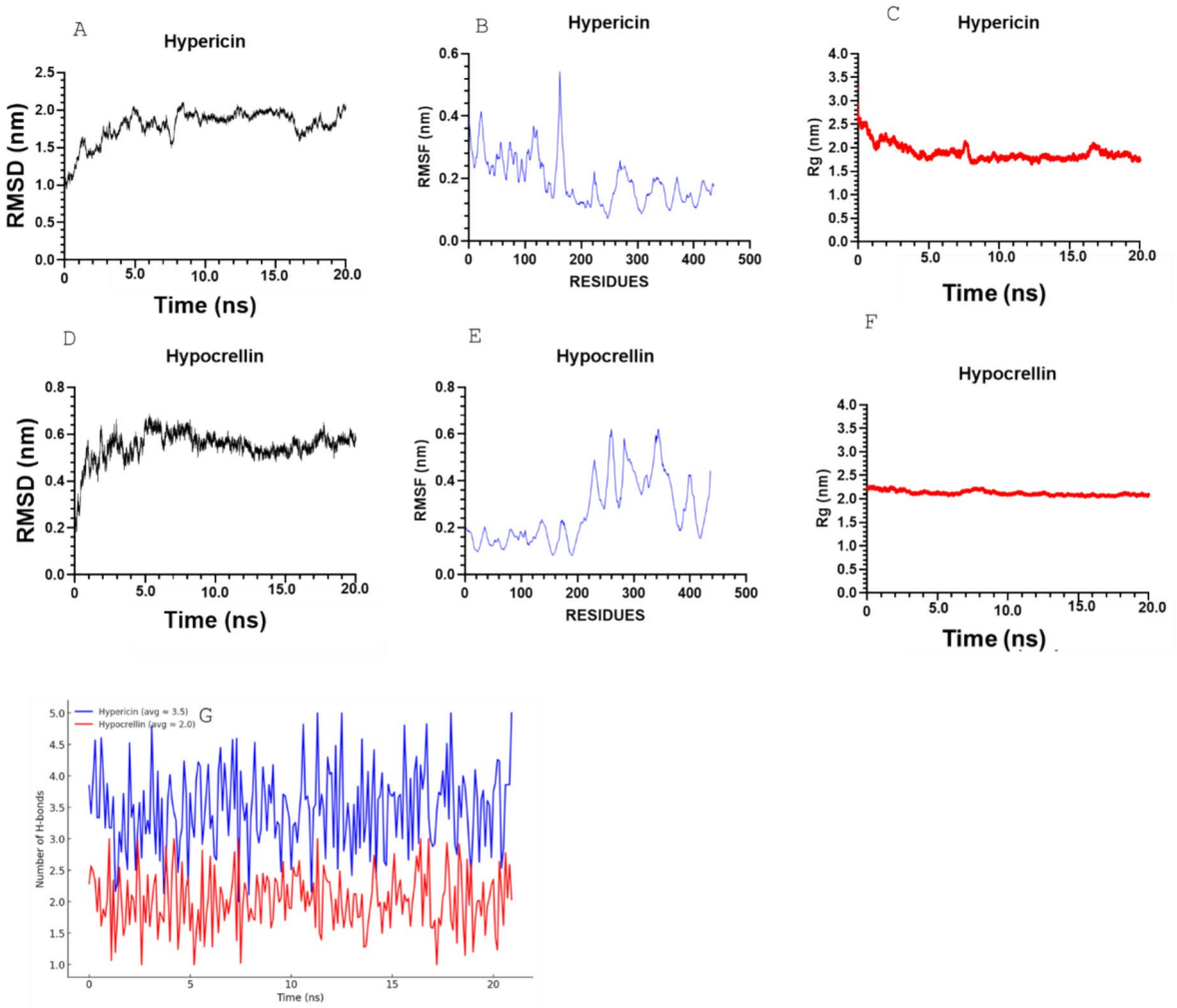

Fig. 5. Molecular dynamics simulation analyses of SGC enzyme complexes. (**A**) RMSD of SGC-Hypericin; (**B**) RMSF of SGC-Hypericin (**C**) Radius of gyration of SGC-Hypericin; (**D**) RMSD of SGC-Hypocrellin. (**E**) RMSF of SGC-Hypocrellin (**F**) Radius of gyration of SGC- Hypocrellin. (**G**) H-bond analysis of both hypericin and hypocrellin in SGC.

Molecular docking analysis of sGC with hypericin and hypocrellin A2

Hypericin: inhibition via H-NOX domain binding

Hypericin's occupation of the H-NOX domain the canonical heme-binding site suggests a direct mechanism of inhibition by interfering with NO binding or the subsequent conformational changes necessary for enzyme activation[24]. By forming stabilizing interactions with residues such as His105, Hypericin likely disrupts the dynamic heme environment essential for allosteric signalling and downstream cyclic GMP (cGMP) synthesis. This domain-specific binding may also influence redox-sensitive processes, particularly under pathological conditions like sepsis or oxidative stress, where the heme group is susceptible to modifications. These findings align with previous reports highlighting the pivotal role of the H-NOX domain in NO-mediated vascular signalling.

Hypocrellin A2: allosteric modulation at the regulatory/catalytic interface

Unlike Hypericin, Hypocrellin A2 binds to a region proximal to the catalytic domain (residues ~ 285–690), suggesting an allosteric mode of action. The formation of hydrogen bonds with Lys284 and Gln309 indicates that Hypocrellin A2 stabilizes a conformation that may impair the interdomain flexibility required for catalytic activation and GTP conversion to cGMP. This region likely serves as a regulatory hub controlling enzyme dynamics rather than substrate or cofactor binding directly. By occupying this strategic location, Hypocrellin A2 could attenuate sGC activity without interfering with NO-heme interactions, enabling partial inhibition or fine-tuned modulation a potentially advantageous mechanism in therapeutic contexts where complete inhibition is undesirable.

Binding free energy analysis

To validate the docking results, we conducted Molecular Mechanics with Generalized Born and Surface Area (MMGBSA) binding free energy calculations for the ligand-enzyme complexes. The analysis revealed that Hypericin and Hypocrellin A2 exhibited particularly strong interactions with soluble guanylate cyclase (sGC), with Hypericin's minimal binding energy reinforcing its potential as an effective therapeutic agent. Howbeit, the MMGBSA method is widely recognized for its effectiveness in estimating binding affinities by decomposing the free energy into various components, including van der Waals, electrostatic, and solvation energies. By averaging over multiple snapshots from molecular dynamics simulations, this approach provides a robust framework for understanding the stability and strength of ligand-receptor interactions[25]. The MMGBSA simulations demonstrate Hypericin's high binding affinity to sGC, which is due to hydrogen-bonding and hydrophobic interactions, emphasizing its therapeutic potential and the importance of computational approaches in drug discovery.

Molecular dynamics

These results reveal significant differences in the dynamic behaviour of the SGC enzyme when bound to Hypericin versus Hypocrellin. The SGC-Hypocrellin complex displays lower and more stable RMSD and RMSF values compared to the SGC-Hypericin complex, signifying that Hypocrellin binding induces a more stable and less flexible enzyme conformation. This rigidity may be favourable for certain enzymatic functions or for maintaining structural integrity under physiological conditions[26]. The SGC-Hypericin complex shows a declining R. g, indicating that its structure becomes more compact during the simulation, potentially as a response to binding-induced stresses or conformational adaptation. Conversely, the SGC-Hypocrellin complex retains a consistent, moderately higher R. g, supporting the idea that its enzyme-ligand structure remains stable and well-packed throughout the simulation. Higher RMSD and RMSF for the Hypericin complex suggest the possibility of partial destabilization or higher flexibility, which could impact enzymatic activity, ligand affinity, or susceptibility to denaturation. The more stable Hypocrellin complex, with its low RMSD/RMSF and steady R. g, could point towards a potentially stronger or more persistent interaction with the SGC enzyme, possibly affecting enzymatic regulation or inhibitor design.

Pharmacokinetic properties

Hypericin demonstrated favourable pharmacokinetic properties characterized by high tissue-binding potential and prolonged half-life. The increased total polar surface area after receptor binding supports its stability and distribution profile, enhancing its therapeutic viability. Comparatively, Hypocrellin A2 exhibited favourable water solubility due to its log P of 4, which promotes bioavailability and renal excretion. These pharmacokinetic profiles align with findings from previous research indicating that natural compounds often possess advantageous absorption and distribution characteristics.

Furthermore, Hypericin's alignment with Lipinski's rule of five suggests it meets essential drug-likeness criteria, a significant advantage over standard inhibitors that frequently violate these parameters[27].

Toxicity assessment

The metabolic profile of Hypericin, a prominent compound in St. John's Wort (Hypericum perforatum), reveals significant interactions with several cytochrome P450 (CYP) enzymes, which are pivotal in drug metabolism. The identification of both active and inactive clusters of interactions provides critical insights into Hypericin's pharmacokinetic behaviour and its potential implications for clinical use. Howbeit, the strong likelihood of interaction between Hypericin and key cytochrome P450 (CYP) enzymes such as CYP1A2, CYP2C9, and CYP2C19 as depicted in Fig. 6, suggests that Hypericin may undergo substantial biotransformation through these pathways. This biotransformation could significantly influence the compound's bioavailability and half-life, leading to variations in its therapeutic effectiveness. Given that these CYP enzymes are responsible for metabolizing a wide range of medications, the potential for drug-drug interactions is a notable concern. Co-administration of Hypericin with drugs that are substrates for these enzymes could result in altered plasma concentrations of those medications, potentially diminishing their efficacy or increasing the risk of adverse effects. Previous studies have indicated that St. John's Wort extracts, which contain Hypericin, can inhibit the activities of several CYP enzymes, including CYP1A2 and CYP2C9, thereby raising concerns about possible pharmacokinetic interactions with co-administered drugs[28,29]. Moreover, the moderate interaction probabilities associated with CYP3A4 and CYP2D6 further underscore the importance of considering Hypericin's impact on drug metabolism. Even moderate interactions can lead to clinically relevant changes in pharmacokinetics, necessitating careful monitoring when Hypericin is used alongside other medications. Research has shown that while Hypericin may not significantly induce CYP3A4 activity, it can still influence the metabolism of drugs processed by this enzyme[30–32]. The toxicological assessment of Hypericin indicates a predicted LD50 of 1000 mg/kg, placing it in Toxicity Class 4 according to the Globally Harmonized System (GHS). This classification suggests that while Hypericin can be harmful if ingested in significant amounts, it is generally considered to have a lower toxicity profile compared to more hazardous substances. The relatively wide therapeutic window indicated by this classification is encouraging for its potential therapeutic applications; however, it also highlights the necessity for careful dose management to mitigate any risk of adverse effects. Additionally, the assessment reveals low probabilities for neurotoxicity and carcinogenicity, reinforcing the notion that Hypericin may be a safer option for therapeutic use. This low-risk profile is particularly important in oncology and other therapeutic areas where safety is paramount. The absence of significant toxicological risks associated with cardiac or immune function further supports its potential as a therapeutic agent. he findings from this metabolic and toxicological profiling underscore the need for further research to validate these results through experimental studies and clinical trials. Understanding the specific mechanisms by which Hypericin interacts with various CYP enzymes will be crucial

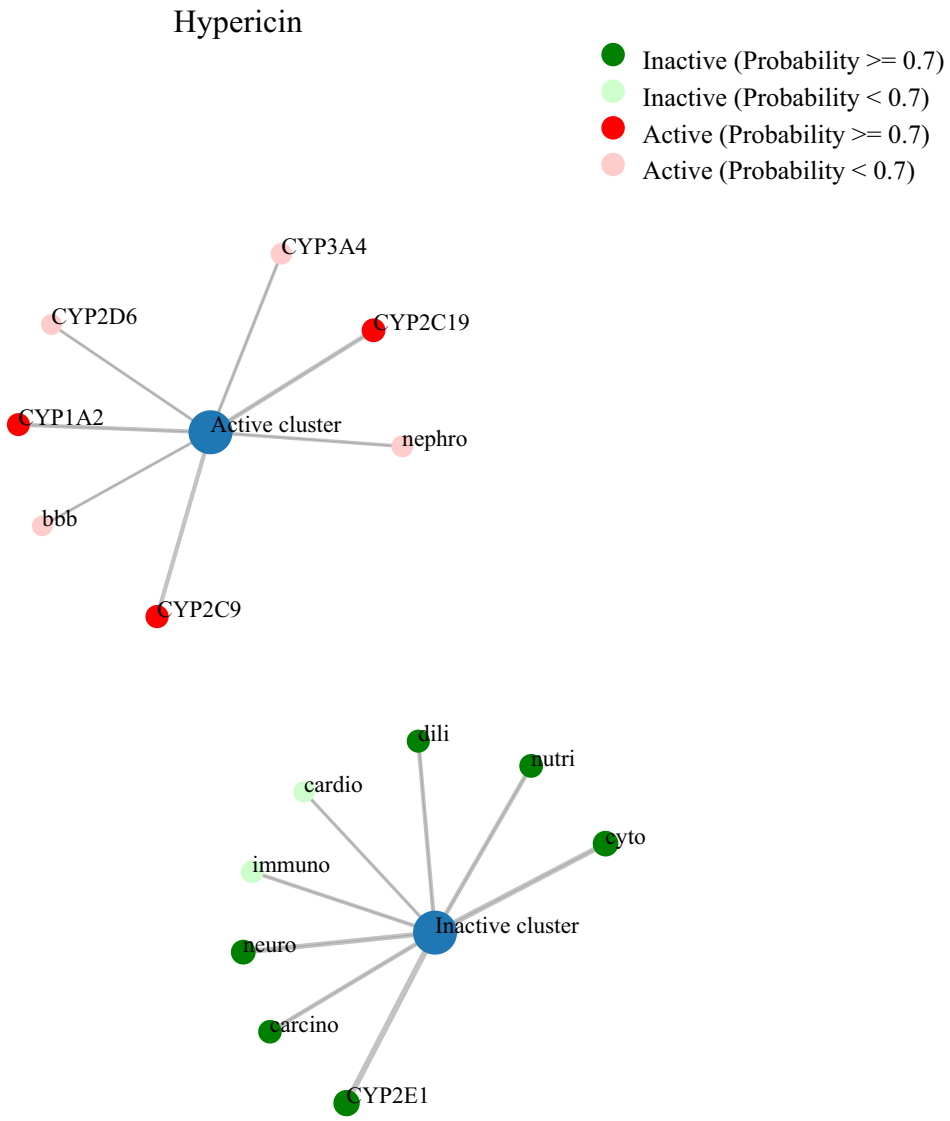

Fig. 6. Network chart of hypericin's predicted toxicological profiles.

for predicting its behaviour in clinical settings. Additionally, exploring the implications of these interactions on patient safety and drug efficacy will be vital as Hypericin continues to gain attention in pharmacological research.

Conclusion

Our findings position Hypericin as a promising candidate for treating sepsis-induced vasoplegia by targeting sGC to mitigate multi-organ failure. The study emphasizes the value of natural compounds in drug discovery and the efficacy of computational methods in identifying viable therapeutic candidates. Future validation through in vitro and in vivo studies is essential to confirm these findings and explore Hypericin's full therapeutic potential. This research contributes significantly to the ongoing discourse surrounding sepsis treatment strategies and highlights the importance of integrating computational drug design into modern pharmacological research. By focusing on natural compounds like Hypericin, we may pave the way for innovative therapies addressing complex pathologies such as sepsis while minimizing toxicity risks associated with traditional pharmaceuticals.

Data availability

The datasets generated and/or analysed during the current study are available from the corresponding author on reasonable request.

Received: 11 January 2025; Accepted: 17 September 2025
Published online: 22 October 2025

References

1. Liu, Z. et al. From immune dysregulation to organ dysfunction: understanding the enigma of Sepsis. *Front. Microbiol.* **15**, 1415274 (2024).
2. Rhodes, A. et al. Surviving Sepsis Campaign: International Guidelines for Management of Sepsis and Septic Shock: 2016. *Crit. Care Med.* **45**(3), 486–552 (2017).
3. Fajgenbaum, D. Storm June CH. *Cytokine N. Engl. J. Med.* **383**(23), 2255–2273 (2020).
4. Martin, G. S., Mannino, D. M., Eaton, S. & Moss, M. The epidemiology of sepsis in the United States from 1979 through 2000. *N. Engl. J. Med.* **348**(16), 1546–1554 (2003).
5. Organization WH. WHO calls for global action on sepsis-cause of 1 in 5 deaths worldwide. (2020).
6. Angus, D. C. & Van der Poll, T. Severe sepsis and septic shock. *N. Engl. J. Med.* **369**(9), 840–851 (2013).
7. Petros, A., Bennett, D. & Vallance, P. Effect of nitric oxide synthase inhibitors on hypotension in patients with septic shock. *Lancet* **338**(8782–8783), 1557–1558 (1991).
8. Seymour, C. W. et al. Assessment of clinical criteria for sepsis: for the third international consensus definitions for sepsis and septic shock (Sepsis-3). *JAMA* **315**(8), 762–774 (2016).
9. Singer, M. et al. The third international consensus definitions for sepsis and septic shock (Sepsis-3). *JAMA* **315**(8), 801–810 (2016).
10. Julou-Schaeffer, G. et al. Loss of vascular responsiveness induced by endotoxin involves L-arginine pathway. *Am. J. Physiol. Heart Circ. Physiol.* **259**(4), H1038–H1043 (1990).
11. Kilbourn, R. G. et al. Reversal of endotoxin-mediated shock by NG-methyl-L-arginine, an inhibitor of nitric oxide synthesis. *Biochem. Biophys. Res. Commun.* **172**(3), 1132–1138 (1990).
12. Rees, D., Cellek, S., Palmer, R. & Moncada, S. Dexamethasone prevents the induction by endotoxin of a nitric oxide synthase and the associated effects on vascular tone: an insight into endotoxin shock. *Biochem. Biophys. Res. Commun.* **173**(2), 541–547 (1990).
13. Tang, D., Kang, R., Coyne, C. B., Zeh, H. J. & Lotze, M. T. PAMP s and DAMP s: Signal 0s that spur autophagy and immunity. *Immunol. Rev.* **249**(1), 158–175 (2012).
14. Liu, R., Kang, Y. & Chen, L. Activation mechanism of human soluble guanylate cyclase by stimulators and activators. *Nat. Commun.* **12**(1), 5492 (2021).
15. Farah, C., Michel, L. Y. & Balligand, J.-L. Nitric oxide signalling in cardiovascular health and disease. *Nat. Rev. Cardiol.* **15**(5), 292–316 (2018).
16. Sandner, P. From molecules to patients: exploring the therapeutic role of soluble guanylate cyclase stimulators. *Biol. Chem.* **399**(7), 679–690 (2018).
17. Czaikoski, P. G., Nascimento, D. B. C., Spiller, F. & Cunha, F. Q. Heme oxygenase and soluble guanylate cyclase mediate the neutrophil migration failure to the lung in severe sepsis induced by pneumonia. *Crit. Care* **13**(3), P24 (2009).
18. Fernandes, D. et al. Late, but Not Early, Inhibition of Soluble Guanylate Cyclase Decreases Mortality in a Rat Sepsis Model. *J. Pharmacol. Exp. Ther.* **328**(3), 991–999 (2009).
19. Cauwels, A. et al. Protection against TNF-Induced Lethal Shock by Soluble Guanylate Cyclase Inhibition Requires Functional Inducible Nitric Oxide Synthase. *Immunity* **13**(2), 223–231 (2000).
20. Zhang, J. et al. Hypericin: Source, Determination, Separation, and Properties. *Sep. Purif. Rev.* **51**(1), 1–10 (2022).
21. Zhang, X. et al. Advancements and Future Prospects in Hypocrellins Production and Modification for Photodynamic Therapy. *Fermentation.* **10**(11), 559 (2024).
22. Pecchiari, M. et al. Cardiovascular responses during sepsis. *Compr. Physiol.* **11**(2), 1605–1652 (2021).
23. Kimmoun, A., Ducrocq, N. & Levy, B. Mechanisms of vascular hyporesponsiveness in septic shock. *Curr. Vasc. Pharmacol.* **11**(2), 139–149 (2013).
24. Alamami, A. et al. Clinical Outcomes of Angiotensin II Therapy in Vasoplegic Shock: A Systematic Review and Meta-Analysis. *Life.* **14**(9), 1085 (2024).
25. Petrova O. *Regulation, activation, and deactivation of soluble guanylate cyclase and NO-sensors* (Doctoral dissertation, Université Paris Saclay (COmUE)).
26. Forouzesh, N. & Mishra, N. An effective MM/GBSA protocol for absolute binding free energy calculations: A case study on SARS-CoV-2 spike protein and the human ACE2 receptor. *Molecules* **26**(8), 2383 (2021).
27. Minić, S., Annighöfer, B., Brûlet, A., Combet, S. Stability of food proteins at high pressure conditions. *InSerbian Biochem. Soc. Twelfth Conf.* 59 (2023).
28. da Silva, C. P., das Neves, G. M., Poser, G. L., Eifler-Lima, V. L. & Rates, S. M. In silico prediction of ADMET/drug-likeness properties of bioactive phloroglucinols from Hypericum genus. *Med. Chem.* **19**(10), 1002–1017 (2023).
29. Obach, R. S. Inhibition of human cytochrome P450 enzymes by constituents of St. John's Wort an herbal preparation used in the treatment of depression. *J. Pharmacol. Exp. Ther.* **294**(1), 88–95 (2000).
30. Henderson, L., Yue, Q. Y., Bergquist, C., Gerden, B. & Arlett, P. St John's wort (Hypericum perforatum): drug interactions and clinical outcomes. *Br. J. Clin. Pharmacol.* **54**(4), 349–356 (2002).
31. Komoroski, B. J. et al. Induction and inhibition of cytochromes P450 by the St. John's wort constituent hyperforin in human hepatocyte cultures. *Drug Metabol. Dispos.* **32**(5), 512–518 (2004).
32. Hakkola, J., Hukkanen, J., Turpeinen, M. & Pelkonen, O. Inhibition and induction of CYP enzymes in humans: an update. *Arch. Toxicol.* **94**(11), 3671–3722 (2020).

Acknowledgements

We deeply thank Abuzor Mohamed Mohyeldin Khalil for his invaluable guidance and expertise throughout this study.

Author contributions

Yousif Ali Ahmed Suleiman is the principal investigator and the main supervisor is Yassir Ali Almofti formulated the research idea, screened the natural drug from PubChem, defined the control ligand and the structure of the tested receptor, performed all the experiments, evaluated the data and prepared the final manuscript. Abuzor Mohamed Khalil helped in the experimental procedures and data analysis to prepare the main manuscript.

Funding

This work was supported by the Deanship of Scientific Research, Vice Presidency for Graduate Studies and Scientific Research, King Faisal University, Saudi Arabia, under the Annual Research Track (KFU253326).

Declarations

Competing interests
The authors declare no competing interests.

Additional information
Correspondence and requests for materials should be addressed to Y.A.A.

Reprints and permissions information is available at www.nature.com/reprints.

Publisher's note Springer Nature remains neutral with regard to jurisdictional claims in published maps and institutional affiliations.